



Applying GPR and 2D ERT for Shallow Landslides Characterization: A Case Study

Biljana Abolmasov, Aleksandar Ristić, and Miro Govedarica

Abstract

We present a procedure to estimate the characteristics of small shallow landslides based on the application of ground penetrating radar (GPR) and 2D electrical resistivity tomography (ERT). Existing procedures based on either conventional or non-invasive geophysical methods, observe almost exclusively large and deep landslides. Verification has been done on a small shallow landslide in the village of Vinča, near Belgrade, Serbia. The proposed procedure is realized in two simultaneous steps. First, from high resolution raw data obtained by GPR survey, soil horizons inside and near landslide body are estimated up to 4 m deep. The rupture surface is defined and its depth is estimated at 1.7 m. Second, ERT technology confirmed and integrated the results obtained by GPR survey. Main advantages of proposed procedure are efficiency and applicability for small shallow landslides whose number and impact on environment is dominant.

Keywords

Shallow landslides • Ground penetrating radar • 2D resistivity tomography

Introduction

The conventional methods of landslides investigations are based on engineering geological mapping and in most cases combined with borehole drilling, standard penetration test (SPT) and laboratory methods. Therefore, conventional methods are expensive and relatively slow, whereas the results of analysis are based on processing the limited range of subsurface data (Bichler et al. 2004). These disadvantages may be overcome by combined or independent application of non-invasive geophysical methods whose expansion follows the development of modern techniques and instruments

(McGuffey et al. 1996). Simultaneously with the development of these methods, the possibilities of their application in detailed research of landslides were analysed (Hack 2000; Bichler et al. 2004). These analyses were carried out almost exclusively for large landslides with the sliding depth bigger than 20 m, and showed that ERT technology is rather appropriate in these conditions (Godio and Bottino 2001; Lapenna et al. 2003; Xiujun et al. 2005; Friedel et al. 2006; Marescot et al. 2008; Göktürkler et al. 2008). In terms of large deep landslides, GPR technology has been used only to confirm the results of ERT technology, due to maximum penetration depth of electromagnetic (EM) waves and survey site accessibility (Bichler et al. 2004; Bruno and Marillier 2000). Considering that the main goal of the research is to determine characteristics of small shallow landslides with the sliding depth in the range up to 5 m and then the application of GPR technology, which is characterized by swift and completely non-invasive acquisition of high resolution data, becomes very appropriate (Ristić et al. 2009). Taking into account objective possibilities of non-invasive geophysical methods, they are rarely carried out independently.

B. Abolmasov (✉)
Faculty of Mining and Geology, University of Belgrade, Djusina 7,
Belgrade, Serbia
e-mail: biljana@rgf.bg.ac.rs

A. Ristić • M. Govedarica
Faculty of Technical Sciences, University of Novi Sad,
Novi Sad, Serbia

More often, they are used in combination with other methods and then correlation of obtained results is carried out. Such integrated geophysical approach of using different methods combined with traditional methods of research is described in various papers (Sass et al. 2008; Naudet et al. 2008). Advantages and disadvantages of using geophysical methods in geomorphological studies are described on various examples by Schrott and Sass (2008).

On the basis of previously mentioned points, it can be concluded that recent results of landslide analysis point to the integrated approach which involves different technologies of active remote sensing. Also, the analysis of small shallow landslides was rarely tackled in literature, while the GPR technology was not applied significantly.

Since small shallow landslides are numerous and their impact on environment is considerable, this paper aims to represent new procedure for defining their characteristics. The presented procedure involves combined application of GPR and ERT technologies and it has been verified on the given landslide.

During the research the emphasis was put on non-invasive geophysical methods since the landslide has specific position and geometry. Due to capabilities of non-invasive geophysical methods for the landslide research (Bichler et al. 2004) field work was conducted during the summertime (July 2009), in a dry period, after the period of heavy precipitation in the previous winter and spring which reactivated the landslide. Results presented in this paper clearly show that in case of small shallow landslides applied geophysical methods give reliable data on the structure of a landslide body and the spatial disposition of the rupture surface.

Materials and Methods

The integrated geophysical research was carried out on the landslide located 14 km southeast of Belgrade, in the village of Vinča, on the right bank of the Danube (Fig. 1). The right valley bank of the Danube is characterized by hills (altitude of 80–130 m) and numerous deep landslides whose feet reach the Danube (Rokić 1997). The general geological settings of study area includes continual surface layer of diluvium (dl) with the thickness of 0.2–0.5 m and beneath it there is loess (Q) with the thickness of 0.5–2.0 m with traces of secondary carbonate sediments (Jevremović and Kuzmić 2001). The bedrock consists of Sarmatian sand (M_3^1), brownish marls (M_3^1GL) and grey marls (M_3^1L).

The analysed landslide has the dimensions of 50 × 40 m and it is situated in the middle of the Danube slope above the local road and three private residential objects that are directly endangered by the landslide (Figs. 1 and 2).

The landslide is on the private property and due to the specific terrain configuration and the problems with the owners of nearby properties it is almost impossible to reach the body of the landslide equipped with drill tools and tools for SPT measurements.

The landslide activated in March 2008 was triggered by heavy rainfall and slope indentation. Indentation was done while building residential objects. First reactivation occurred in March 2009, also triggered by heavy rainfall. Second reactivation occurred in late December 2009 and was triggered by instant snow melting (Fig. 2). According to Cruden and Varnes (1996), this landslide can be classified as shallow retrogressive and active landslide, very slow to slow, in the phase of active movement. The main scarp, with the height of 1.7 m is obvious with the visible zone of mass deficit. Lithological composition of the landslide comprises a thin diluvium with the thickness up to 0.3 m, loess with the thickness of 1–1.5 m and bedrock consisted of Sarmatian laminated well-compacted sand with weathered marls (Fig. 3).

Ground Penetration Radar Scanning

The data acquisition was done in July 2009, with GSSI SIR3000 system. The formation of radargram was carried out using antennas with central frequency 200, 400 and 900 MHz and a high scan resolution of 1,024 samples/scan, and 100 scan/m. The maximum scanning depth of 4 m was achieved by antenna with the central frequency 200 MHz taking into consideration soil structure in the landslide body and capabilities of used antenna. GPR calibration, in terms of determining the dielectric constant of soil was done according to known lithological structure of main scarp area (Ristić et al. 2007, 2009). Figure 4 shows the layout and numbering of radargrams in order of acquisition (labels from F029 to F059), with defined acquisition parameters: the direction of antenna motion (marked by arrow), antenna frequency (200, 400 and 900 MHz) and measuring location characteristics. Points used to georeference the radargrams were measured using two Trimble 5800 Global Positioning System (GPS) rovers in Real-Time Kinematic (RTK) mode (first covers the points 01–16, while the second covers the points p001–p011). The set of characteristic points for radargram georeferencing contains start and end point. Radargram post-processing, conducted in software package RADAN, included determination of time zero distance (distance from the antenna centre to the soil surface), and the application of several digital signal processing algorithms for reflected signals processing. It was done to obtain a clear view of all structural characteristics of landslides (Ristić et al. 2007, 2009).

Fig. 1 Geographical position of study area

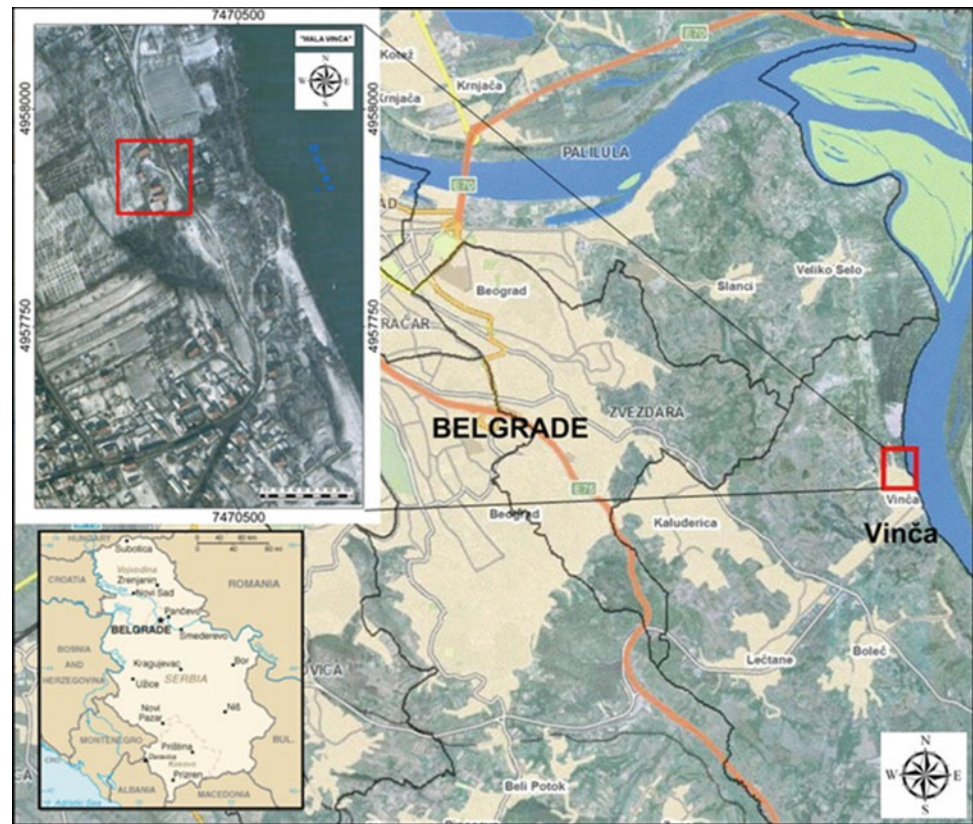


Fig. 2 Landslide Vinča (Photo December 2009)



Fig. 3 Weathered Sarmatian marls (Photo December 2009)

Electrical Resistivity Tomography

In addition to the acquisition by GPR, another profile of detailed ERT scanning was done and its location is shown by a discontinuous line in Fig. 4. The equipment used for data acquisition was ABEM SAS 300B with sensitivity of 0.01 mV. The length of the profile was 45 m, and there was 113 points at 6 depth levels. The distance between two measuring points (step) was 2 m. The total depth was

approximately 4 m. The processing of measured data was conducted by software packet RES2DINV. The complete profile was carried out by the combination of Wenner-Schlumberger array electrodes. The first depth level was done by Wenner array configuration; the distances between A-M-N-B were equal (2 m), whereas A and B are electrodes for introducing electric current J (mA) into the ground, and M and N are electrodes for measuring the difference of electric potential ΔV (mV). From level 2 to level 6 electrode

Fig. 4 Disposition of GPR and ERT profiles

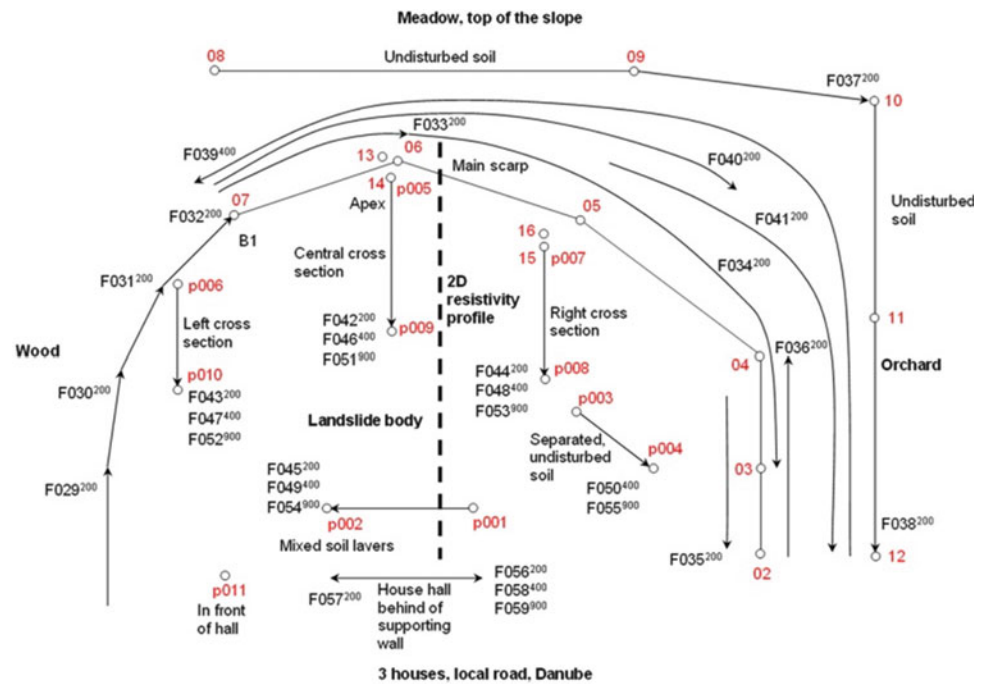
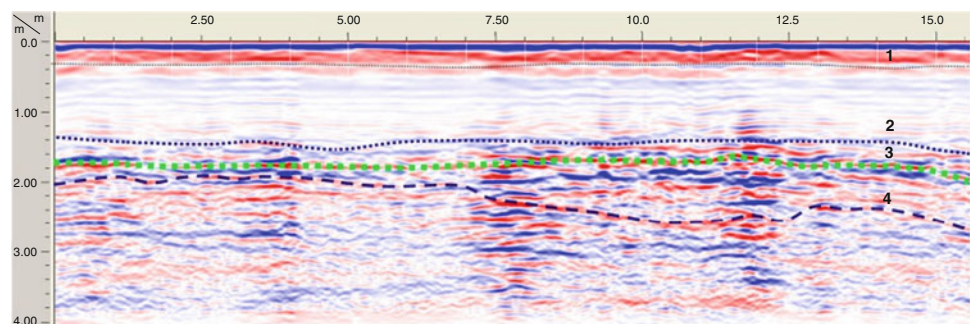


Fig. 5 Interpretation of the radargram F032



configuration. Schlumberger was used where the distance M-N remains the same (2 m) while the distance between current electrodes A-B successively increases (10, 14, 18, 22 and 26 m). The measurements on the points consisted of placing M and N at a 2-m distance, and a series of measuring $\Delta V/J$ ratio at the rising distances A and B from 6 m (Wenner, 2-2-2) to 26 m (Schlumberger, 12-2-12, for last sixth level). In case of Schlumberger configuration A-M-N-B, A-M and N-B, the distances between electrodes increased successively (2, 4, 6, 8, 10 and 12 m).

Results and Discussion

Using technologies of GPR and ERT, 31 profiles are generated: 30 GPR and 1 ERT profile. Several GPR profiles that characterize the most important features have been selected for discussion. The interpretation and relation of geophysical data to lithological data are then presented in the following.

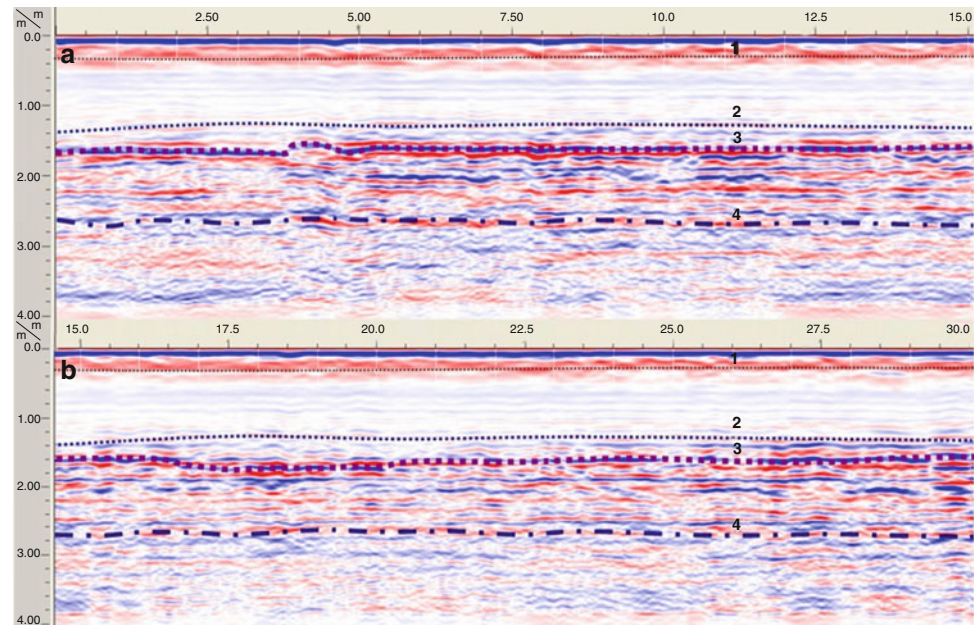
The disposition of the radargrams F032, F033 and F034 and its starting and ending points (formed in nearby, undisturbed terrain) is shown in Fig. 4. Lithological elements that can be found in the landslide body are noticed in these radargrams as well. The marks from 1 to 4 define the position of borders between soil horizons in these radargrams.

Ground Penetrating Radar Results (GPR)

Radargram F032, 16 m¹ long, is formed in undisturbed terrain, about 1 m parallel to the edge of the right side scarp (Fig. 4). The coordinates of the beginning of radargram F038 (0 m¹) are not measured by GPS (surrounded by trees), and the end of radargram corresponds to the point 07 (16 m¹). The changes in terms of the phase inversion of reflected signal and disorder of the structure range from 7 m¹ to 16 m¹ (Fig. 5). The changes are especially visible from 7 m¹ to 12 m¹.

Radargram F033, 7 m¹ long, is formed in undisturbed terrain left from the head scarp apex. The beginning of F033

Fig. 6 Interpretation of radargram F034



radargram (0 m^1) corresponds to the coordinates of the point 07 (the position of the scanner B1), and the end of the radargram corresponds to the point 06 (7 m^1) – head scarp apex (Fig. 8a). The abscissa of the radargram F033 defines the resolution of generating scans where the achieved resolution is 1scan/1 cm. The given resolution is the same for all shown radargrams. Scan 390 from radargram F033 is represented with oscilloscope preview of reflected signal with clearly visible borders between soil horizons.

Since it was possible to see a part of soil horizons on the main scarp apex, they served as a solid basis for interpreting geophysical data. Therefore, the radargram F033 is formed directly above the scarp, so geophysical parameters can be defined and correlation between borders in radargram and visible soil horizons is established. Figure 8b shows a visual representation of the borders 2 and 3 which served as a basis for recalibration of a device and defining dielectric constant $\epsilon_R = 28$ (Saarenketo 1998).

Radargram F034, 33 m^1 long, is formed in undisturbed terrain (in time of acquisition) and involves the entire left side scarp starting from the head scarp apex (Fig. 4). The beginning of F034 (0 m^1) radargram corresponds to the coordinates of the point 06, 8 m^1 corresponds to the point 05, 24 m^1 to the point 04, and the end corresponds to the point 03 (33 m^1). The changes in terms of phase inversion of reflected signal and disorder of the structure can be seen in a complete radargram (Fig. 8a, b). The changes are especially noticeable from 2 m^1 to 20 m^1 .

The interpretation of the radargrams F032, F033 and F034 (Fig. 5, 6 and 8)

- Soil horizon from the surface to the border 1 – from 0 to 30 cm – humificated loess diluvium, dark brown, dry

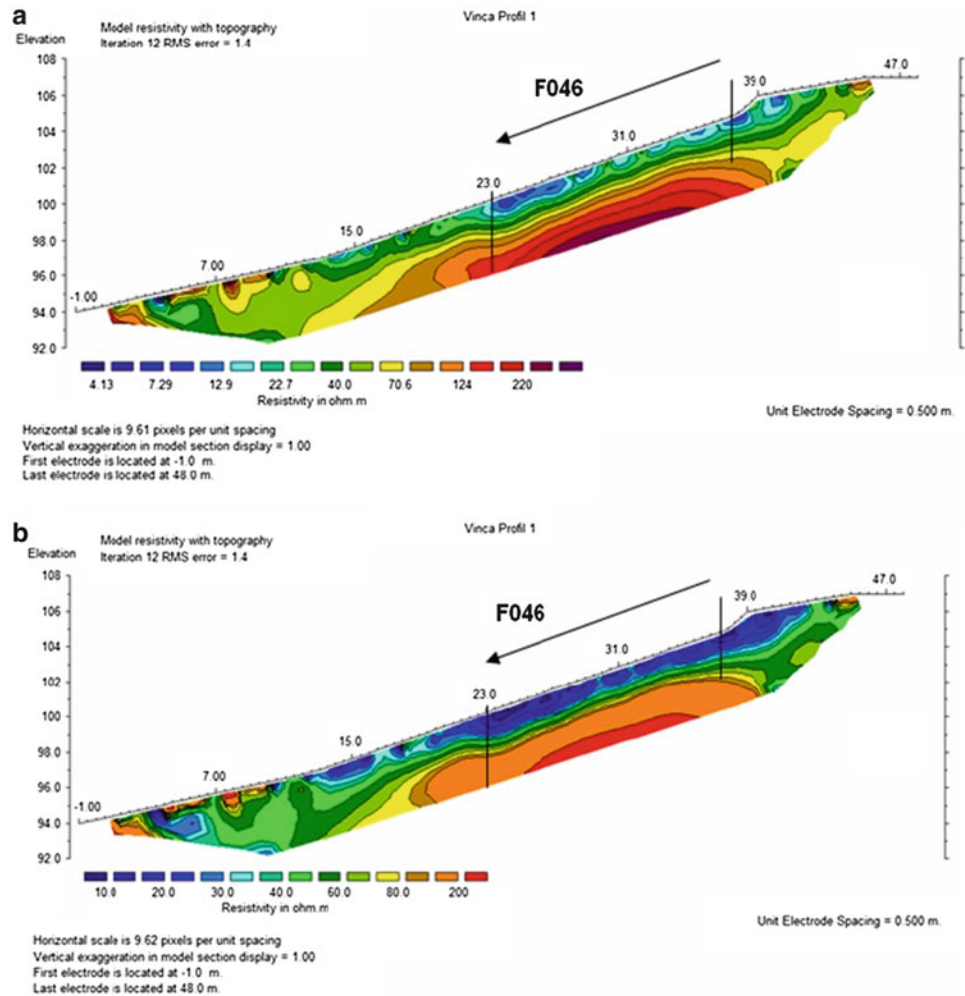
- Soil horizon between borders 1 and 2 – from 30 to 135 cm – loess diluvium, pale brown, dry with variable amount of carbonates
- Soil horizon between borders 2 and 3 – from 135 to 170 cm – incoherent sand, pale brown
- Soil horizon between borders 3 and 4 – from 170 to 210 cm – on F032, that is, 260 cm on F034 – weathered marls; at 170 cm there is maximum reflected amplitude, probably clay sediments but also distorted structures and air-filled fractures, which was confirmed after the second reactivation of landslide in December 2009 (Fig. 9)
- Soil horizon beneath border 4 – high reflection amplitude, probably weak consolidated sand, no phase inversion and a small amount of moisture.

Radargram F046, 13.6 m^1 long, is formed in the landslide body starting from the head scarp apex to the centre of the landslide body. Beginning of radargram F046 (0 m^1) corresponds to the point p005, and the end of radargram corresponds to the point p009 (13.6 m^1). The trace of radargram F046 overlaps the part of ERT profile, where the starting point of radargram p005 corresponds to 37 m^1 of ERT profile, and the ending point of radargram p009 corresponds to 23 m^1 of ERT profile. Since height of the starting point p005 is 113.9 m above mean sea level and the end point p009 is at 109.4 m, then the difference in height of the profile is 4.5 m.

The comparative analysis of geophysical data from common parts of the radargram trace F046 and ERT profile showed an excellent correlation. It is explained in more detail when interpreting the results from ERT profile.

The labels 1 and 2 define the position of interpreted borders on the radargram F046:

Fig. 7 Interpretation of ERT profile



- Soil horizon from the surface to the border 1 – from 0 to 65 cm – homogenous lithological composition and structure
- Soil horizon between borders 1 and 2 – from 65 to 120 cm – disorder in structure and phase inversion of reflected signal
- Soil horizon beneath border 2 – completely disordered structure with a high percentage of clay and significant attenuation of signal. Possible surface of rupture is expected in this soil horizon, but deeper than maximum penetration depth of EM wave.

ERT Profile: Central Cross Section in Landslide Body

In the raw ERT profile (Fig. 7a) three resistivity units can be identified. First, there is a clearly visible unit with a low specific electrical resistivity with values between 10 and 20 Ωm (marked with shades of blue colour). This unit reaches the depth of 65 cm and it can be related to moved diluvium and loess sediments and incoherent sands.

Second, resistivity unit with values between 20 and 70 Ωm (in ERT profile marked with shades of green), can be related to the landslide body consisting of moved diluvium, loess and sand, and at the bottom there is weathered marls where, at the depth of maximum 170 cm, the surface of rupture was formed.

The third, clearly identified resistivity unit in ERT profile was coloured in yellow to the nuances of red with corresponding resistivity ranging from 70 to 250 Ωm . This unit most probably corresponds to weak consolidated sand that can be seen in immediate adjacency to the landslide on a smaller vertical cut. Also, there are traces of clay. In ERT profile can be distinguished the debris, that is, the material which is deposited from 0 m¹ to 10 m¹ of the profile length. All the results are defined in the raw ERT profile (Fig. 7a) and they become more visible after re-interpretation considering identified resistivity units (Fig. 7b).

Comparing interpretation results of the radargram F046 and ERT profile it can be noticed that border 1 on radargram corresponds to resistivity unit 1 on ERT profile. Also, border 2 on radargram corresponds to light green colour from

Fig. 8 Interpretation of radargram F033 on the head scarp apex

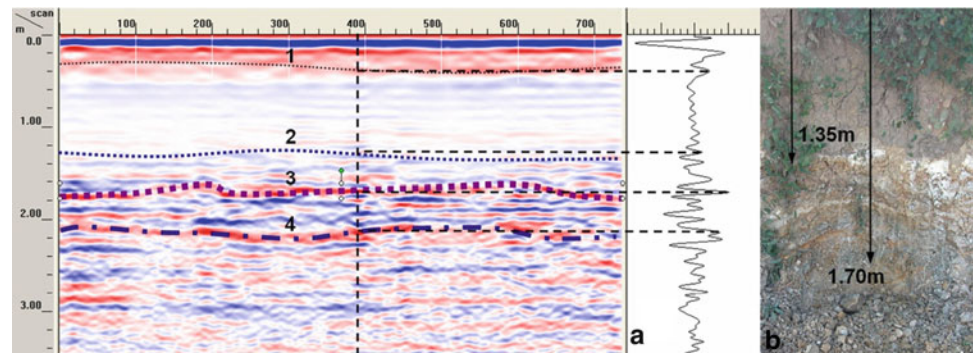


Fig. 9 Sliding surface (Photo December 2009)

resistivity unit 2 on ERT profile. It means, in this case, these two methods resulted in well correlated data (Fig. 7a, b).

ERT profile is perpendicular to head scarp and crosses radargrams F033 and F034. Since there is overlapping zone above head scarp apex it is possible to compare interpretation results of radargrams and profile. There are overt changes in the soil structure in the length of maximum 3 m¹ (from 39 m¹ to 42 m¹ in ERT profile) and to the depth of maximum 170 cm that can be noticed on the radargrams as well. This leads to conclusion that in this zone it is expected to have a further expansion of the landslide. After landslide reactivation in December 2009 this assumption was confirmed. Reactivation occurred in zones of the left side and head scarp. Surface of rupture was revealed at the depth of 170–180 cm (Fig. 9).

Conclusion

The paper presents the procedure to estimate characteristics of small shallow landslides that, in scientific literature, have not been treated appropriately, regarding their number and impact on environment. Proposed procedure is based on the integrated application of active remote sensing technologies (GPR and ERT) whose characteristics are mostly adequate for analysing

the given type of the landslide. The capabilities of the proposed procedure have been successfully verified on a typical example of the landslide in the village of Vinča, near Belgrade, Serbia.

GPR technology was chosen to be the primary one, due to accessibility and dimensions of the landslide, as well as speed and resolution of data acquisition. The comparative analysis of results obtained by GPR and ERT technologies resulted in a more detailed and clearer interpretation of the landslide body structure. GPR scanning enabled the data of high resolution to the maximum depth of 4 m, and the most important results include estimation of the surface of rupture at the depth of 1.70 m, the composition of the landslide body and the prediction of landslide enlargement directions.

The results obtained by proposed procedure may be used as a high-quality input data for shallow landslides mitigation. Due to the widespread presence of this type of landslide, the achieved results can be used as simultaneously as conventional methods.

References

- Bichler A, Bobrowsky P, Best M, Douma M, Hunter J, Calvert T, Burns R (2004) Three-dimensional mapping of a landslide using multi-geophysical approach: the Quesnel Forks landslide. *Landslides* 1:29–40
- Bruno F, Marillier F (2000) Test of high-resolution seismic reflection and other geophysical techniques on the Boup landslide in the Swiss Alps. *Surveys Geophys* 21:333–348
- Cruden DM, Varnes DJ (1996) Landslide types and processes. In: Turner KA, Schuster RL (eds) *Landslides investigation and mitigation*. Special report 247, Transportation Research Board, National Research Council, National Academy Press, Washington DC, pp. 36–75
- Friedel S, Thielen A, Springman SM (2006) Investigation of a slope endangered by rainfall-induced landslides using 3D resistivity tomography and geotechnical testing. *J Appl Geophys* 60:100–114
- Godio A, Bottino G (2001) Electrical and electromagnetic investigation for landslide characterisation. *Phys Chem Earth Part C: Solar Terrest Planet Sci* 26:705–710
- Göktürkler G, Balkaya Ç, Erhan Z (2008) Geophysical investigation of a landslide: the Altındağ landslide site, Izmir (western Turkey). *J Appl Geophys* 65:84–96
- Hack R (2000) Geophysics for slope stability. *Surv Geophys* 21:423–448

- Jevremović M, Kuzmić V (2001) Complex geological map of Belgrade KGK 10 (1:10.000). Geozavod, Beograd
- Lapenna V, Lorenzo P, Perrone A, Piscitelli S, Sdao F, Rizzo E (2003) High resolution geoelectrical tomographies in the study of Giarossa landslide (southern Italy). *Bull Eng Geol Environ* 62:259–268
- Marescot L, Monnet R, Chapellier D (2008) Resistivity and induced polarization surveys for slope instability studies in the Swiss Alps. *Eng Geol* 98:18–28
- McGuffey VC, Modeer VA, Turner KA (1996) Subsurface exploration. In: Landslides investigation and mitigation. Special report 247, Transportation Research Board, National Research Council, National Academy Press, Washington DC, pp. 231–277
- Naudet V, Lazzari M, Perrone A, Loperte A, Piscitelli S, Lapenna V (2008) Integrated geophysical and geomorphological approach to investigate the snowmelt-triggered landslide of Bosco Piccolo village (Basilicata, southern Italy). *Eng Geol* 98:156–167
- Ristić A, Petrovački D, Govedarica M, Popov S (2007) Detection of underground water flows by ground penetrating radar. *Vodoprivreda* 39:228–230 (in Serbian with English abstract)
- Ristić A, Petrovački D, Govedarica M (2009) A new method to simultaneously estimate the radius of a cylindrical object and the wave propagation velocity from GPR data. *Comput Geosci* 35:1620–1630
- Rokić L (1997) Origins of landslides on the right bank of Danube river near Novi Sad. In: International symposium on engineering geology and the environment, Athens, June 23–27, pp 1003–1008
- Saarenketo T (1998) Electrical properties of water in clay and silty soils. *J Appl Geophys* 40:73–88
- Sass O, Bell R, Glade T (2008) Comparison of GPR, 2D-resistivity and traditional techniques for the subsurface exploration of the Öschingen landslide, Swabian Alb (Germany). *Geomorphology* 93:89–103
- Schrott L, Sass O (2008) Application of field geophysics in geomorphology: advances and limitations exemplified by case studies. *Geomorphology* 93:55–73
- Xiujun G, Xiaoyu H, Yonggang J (2005) Forward modelling of different types of landslides with multi-electrode electric method. *Appl Geophys* 2:14–20